Available online at www.sciencedirect.com
ScienceDirect
Journal of the European Ceramic Society 29 (2009) 2757–2763
www.elsevier.com/locate/jeurceramsoc

# Influence of tape cast parameters on texture formation in alumina by templated grain growth

M.D. Snel *, J. van Hoolst, A.-M. de Wilde, M. Mertens, F. Snijkers, J. Luyten

*Materials Department, Flemish Institute for Technological Research (VITO), Boeretang 200, 2400 Mol, Belgium*

Received 12 July 2008; received in revised form 20 February 2009; accepted 7 March 2009
Available online 1 May 2009

**Abstract**

Templated grain growth (TGG) is known as one of the methods to introduce texture in ceramic materials. In order to obtain a highly textured ceramic material with TGG, it is crucial that the seeding particles are well aligned in the green product. Using the shear forces of the tape cast process makes it possible to align seeding particles with shape anisotropy. The influence of different tape cast process parameters on the formation of texture in alumina ceramics using platelet alumina seeding particles has been investigated and quantified. Experiments have been carried out in which the tape cast speed, the deairing time and the gap between doctor blade and carrier film were varied. Further the effect of the seeding particle concentration and the solids loading of the tape cast suspension are investigated. The results are presented in terms of pole figures and lotgering factors.


*Keywords:* Tape casting; $Al_2O_3$; Templated grain growth (TGG)

## 1. Introduction

In order to improve the properties of materials that are typically polycrystalline, it has been proposed to texture the materials microstructure, where achieving the properties of single crystals is the ultimate goal.[1] Since single crystals are in most cases too expensive for practical use, crystallographic texturing of ceramic materials can easily be justified. As such, textured materials are also called the poor man's single crystals, as they can take a distinct position in applications where enhanced material properties are key. A well known example is for instance the application of texturing to piezoelectric ceramics.[1]

There is vast literature on texturing of the microstructure of ceramics, e.g.[2–5] Microstructure texturing has been achieved by pressing or forging, mostly under hot conditions of shape anisotropic particles.[2] An alternative route toward textured ceramics is the so-called templated grain growth (TGG), first described by Seabaugh et al.[6] This processing route readily gives higher degree of texturing compared to hot forging or pressing. In addition more material classes can be processed, and larger flexibility with regard to shaping is possible.

In TGG processing, use is made of single crystals that regulate the grain growth during sintering of a polycrystalline bulk material. In the literature, examples of TGG can be found for, among others, alumina[6,7] and $BaTiO_3$.[8] TGG benefits from the fact that large particles grow preferentially at the expense of finer particles.[9] In order to obtain the desired effect, it is key to make a smart choice for the single crystal seed particles. These are often characterized with shape anisotropy: their morphology displays the typical habitus of the single crystals, e.g. like hexagonal platelets, or rods or needles.[10] Further the template seed particles need to be of sufficient dimensions, compared to the mostly equiaxed matrix particles.

For adequate TGG processing, the template particles are preferentially oriented during processing. This can be obtained by various methods. Examples are the use of anisotropic magnetic susceptibility, making it possible to obtain preferential orientation of particles in a magnetic field and the use of the anisotropic shape, allowing the preferential orientation of such particles when external forces are applied; forces that occur for instance in the process of hot forging or hot pressing as outlined above, or shear forces that are present during specific colloidal shaping processes.

* Corresponding author. Tel.: +32 14 33 5664; fax: +32 14 32 11 86.
*E-mail address:* marcel.snel@vito.be (M.D. Snel).

0955-2219/$ – see front matter © 2009 Elsevier Ltd. All rights reserved.
doi:10.1016/j.jeurceramsoc.2009.03.025

Tape casting is one such process where high shear forces are applied to the suspension upon passing under the so-called doctor blade.[11] In the doctor blade process the suspension is subject to both the pressure flow governed by the height of the liquid column in the reservoir behind the doctor blade and to the drag flow, created by the relative velocity difference between the carrier film and the doctor blade.[12–16] The shear forces in the tape casting process can be held responsible for the alignment of non-equiaxed particles or shape anisotropic particles in green tape cast products. Until recently only the influence of the template concentration[14,17–22] has been studied extensively on the texture, with one study on the influence of carrier speed[14] and viscosity.[14]

In this study we have qualitatively studied the effect of different tape cast parameters, using alumina as a model system. We used a water-based tape cast system for obvious reasons of environmental friendliness and safer use compared to solvent base tape casting.[23–25] Joshi's model[12] was used to explain some of the results found.

## 2. Joshi's model for tape casting

In the tape casting model developed by Joshi,[12] based on other models,[15,16] the shear rate at any location $y$, which is the position between the carrier tape and the doctor gap, is given for power law fluids by

$$K^{1/n}\left(\frac{\partial u}{\partial y}\right) = \left[\left(\frac{\partial P}{\partial x}\right) y - C_1\right]^{1/n} \tag{1}$$

and

$$\eta = K\left(\frac{\partial u}{\partial y}\right)^{n-1} \tag{2}$$

It shows that the shear rate $\partial u/\partial y$ is a function of the viscosity $\eta$ through the constants for power law fluids $K$ and $n$, the gap height $h_0$, and the pressure drop $(\partial P/\partial x)$, which is equal to the hydrostatic pressure $(=\rho g H)$ in the slurry chamber over the length of the doctor blade $L$. If a double doctor blade setup is used, the first gap will control and keep the hydrostatic pressure nearly constant over the second gap, hence the pressure drop over the second blade can be assumed constant.

In Joshi's model the actual velocity distribution is assumed to be part of the velocity profile of the pressure flow as shown in Fig. 1. A constant $\lambda$ is introduced where $2\lambda$ is equal to the ratio between the cross-sectional areas of the imaginary flow channel and the real aperture. For mathematical reasons the boundary conditions are set as described in Fig. 1. Using these boundary conditions, $C_1 = 0$ and the shear rate as function of position $y$ becomes

$$K^{1/n}\left(\frac{\partial u}{\partial y}\right) = \left[\left(\frac{\partial P}{\partial x}\right) y\right]^{1/n} \tag{3}$$

and the shear stress

$$\tau = K\left[\frac{\partial u}{\partial y}\right]^n = K\left[\left(\frac{y(\partial P/\partial x)}{K}\right)^{1/n}\right]^n = Ky\left(\frac{\partial P}{\partial x}\right) \tag{4}$$

The average shear stress can now be calculated by

$$\tau_{average} = \frac{\int_{-\lambda h_0}^{-(\lambda_0-1)h_0} y(\partial P/\partial x)\partial y}{-\lambda h_0 - (-(\lambda_0-1)h_0)} = -\left(\frac{\partial P}{\partial x}\right)\frac{h_0(2\lambda-1)}{2} \tag{5}$$

The constant $\lambda$ can be calculated a priori using the velocity profile obtained by integrating the equation for the shear rate

$$K^{1/n}u + C_2 = \frac{[(\partial P/\partial x)y]^{(1/n)+1}}{(\partial P/\partial x)((1/n)+1)} \tag{6}$$

and using the boundary condition $u = 0$ at $y = -\lambda h_0$ giving

$$u = \frac{[(\partial P/\partial x)y]^{(1/n)+1} - [-\lambda h_0(\partial P/\partial x)]^{(1/n)+1}}{K^{1/n}(\partial P/\partial x)((1/n)+1)} \tag{7}$$

Since $u$ is equal to the carrier tape speed $u_c$ at $y = -h_0(\lambda - 1)$, $\lambda$ can now be solved through

$$u_c = \frac{[-h_0(\partial P/\partial x)(\lambda-1)]^{(1/n)+1} - [-\lambda h_0(\partial P/\partial x)]^{(1/n)+1}}{K^{1/n}(\partial P/\partial x)((1/n)+1)} \tag{8}$$

where all constants, except $\lambda$, are set or can be measured prior to tape casting.

After determining $\lambda$ through Eq. (8), Eq. (5) will be used to determine the influence of the average shear rate for each experiment on the lotgering factor.

## 3. Experimental

A typical preparation of a tape cast slurry uses 110 g of alumina powders of which a specified part are platelets, e.g. 16%. Amounts of deionised water, dispersant, $Al_2O_3$ powder (CT3000 SG, Alcoa, average diameter ~0.7 μm), $Al_2O_3$ platelets (Alusion, Antaria, average diameter ~3 μm, thickness

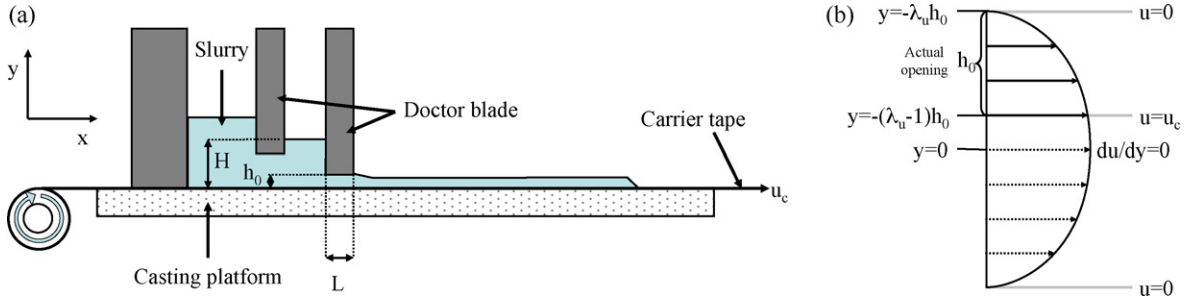


Fig. 1. (a) Tape casting model as used by Joshi and (b) the fluid flow in an imaginary channel for the case where $\lambda > 1.0$, which is mainly applicable in our work. The other cases are described in Ref. 12.

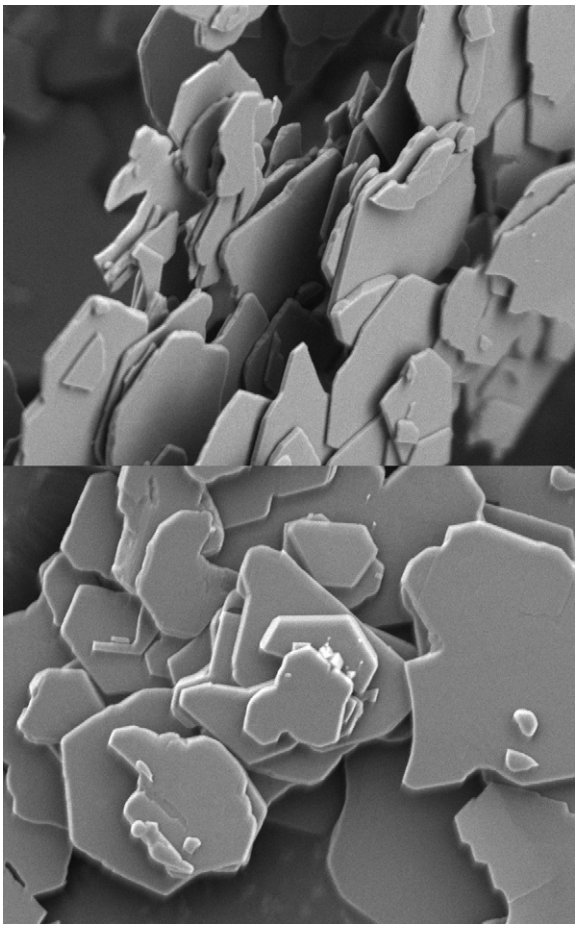

Fig. 2. SEM images of the Alusion platelet particles. Image width is 19 μm. (SEM, Jeol JSM-840A, Japan). The particles have an average diameter of ~3 μm and a thickness of ~0.1 μm.

~0.1 μm, shown in Fig. 2) and ~400 g milling balls (9 mm YSZ) are added together in a ~0.5 l polyamide jar. In order to keep the platelets intact, only gentle ball milling (Fritsch Pulverisette, setting 4, ~120 rpm) was used for 5 min to break the agglomerates and disperse the powder. SEM confirmed the template particles were intact after casting.

In the next step water based latex binder, plasticizer and antifoaming agent were added to the mixture to yield the final slurry composition as given in Table 1. The mixture was gently ball milled for another 5 min. The slurry was typically deaired in a PE flask (250 ml) for 24 h using slow rolling (4 rpm).

Table 1
The base composition of the tape casting slurry.

| Material | Function | Quantity (g) |
|---|---|---|
| Alumina powder (Alcoa CT3000 SG) | Functional phase | 94.8 |
| Alumina platelets (Alusion) | Functional phase and seed particle | 15.2 |
| Water | Suspending medium | 25.0 |
| Darvan C (R.T. Vanderbilt Company) | Dispersant | 2.2 |
| Duramax B-1014 (Rohm&Haas) | Binder | 60.0 |
| PEG 400 (Merck) | Plasticizer | 9.0 |
| DB-310 (Dow Corning) | Antifoaming agent | 1.0 |

Before tape casting, the slurry was poured over a 125 μm sieve to remove any possible large agglomerates. The rheological parameters of the slurries were determined using Haake MARS (Thermo Fisher Scientific, Germany). Typically, double doctor blade tape casting (TCW 1200, Tape Casting Warehouse) was used, using a 0.5 mm front gap height and a 0.6 mm back gap height, a carrier (silicone coated mylar film, Tape Casting Warehouse) speed of 34 cm/min and an underbed temperature of 30 °C. An airflow of ~5 l/min was used to increase the drying rate. Green samples 3 by 4 cm were cut, calcined and sintered at 1650 °C for 4 h in a high temperature furnace (Entech, Sweden). The actual compositions and conditions used are listed in Table 2.

Series of samples were prepared in order to determine the influence of the tape casting process on the degree of texture formation:

(1) the amount of platelets,
(2) the solids loading,
(3) height of the doctor blade,
(4) the carrier speed,
(5) the deairing time.

X-ray diffraction of the samples was performed using Cu-$K_\alpha$ X-ray diffraction (X'Pert Pro, Pananalytical, the Netherlands). The lotgering factor was used to indicate the texture strength. The formula for calculation of the lotgering factor $f$[20,26] is given by

$$f = \frac{p - p_0}{1 - p_0} \tag{9}$$

with

$$p = \frac{\sum I(0\ 0\ l)}{\sum I(h\ k\ l)} \tag{10}$$

where $p$ is the ratio of the peak area under the (0 0 l) peaks and the total area of the peaks in the 20–100° $2\theta$-range. $p_0$ is the same ratio for random orientation. The pole figures were determined for (0 0 6), (0 1 2), (1 0 4), (1 1 0) and (1 1 2) reflections.

## 4. Results and discussion

The overall results for the lotgering factor and the l and average shear stress, as calculated according to Joshi's model,[12] can be found in Table 1.

In Fig. 3 the lotgering factor and the shear stress as a function of the amount of alumina platelets is shown. As expected,[14,17–22] an increased concentration of platelets results in a higher lotgering factor,[26] indicating that the texture in the sintered article increases (Table 3). Increasing the amount of platelets above 8% does not result anymore in a higher lotgering factor, likely due to an increase in template impingement.[9]

Even though a lotgering factor of 1 is to be expected for a fully oriented sample, texture analysis, reveals that a lotgering factor for the (0 0 l) of 0.5 corresponds to a nearly fully (0 0 l) axis oriented sample as shown in Fig. 4, which is conclusive evidence for the presence of texture in the sample. One of the

Table 2
The tape casting parameters for the different experiments.

| # | Platelets (wt%) | Carrier speed (cm/min) | Gap height (mm) | Powder loading (g) | Deairing time (h) |
|---|---|---|---|---|---|
| 1 | 0 | 28 | 0.5 | 110 | 24 |
| 2 | 2 | 28 | 0.5 | 110 | 24 |
| 3 | 4 | 28 | 0.5 | 110 | 24 |
| 4 | 8 | 28 | 0.5 | 110 | 24 |
| 5 | 16 | 28 | 0.5 | 110 | 24 |
| 6 | 16 | 11 | 0.5 | 110 | 0 |
| 7 | 16 | 22 | 0.5 | 110 | 0 |
| 8 (=6) | 16 | 28 | 0.5 | 110 | 24 |
| 9 | 16 | 34 | 0.5 | 110 | 0 |
| 10 | 16 | 45 | 0.5 | 110 | 0 |
| 11 | 16 | 56 | 0.5 | 110 | 0 |
| 12 | 16 | 45 | 0.2 | 110 | 0 |
| 13 | 16 | 45 | 0.3 | 110 | 0 |
| 14 | 16 | 45 | 0.4 | 110 | 0 |
| 15 (=10) | 16 | 45 | 0.5 | 110 | 0 |
| 16 | 16 | 45 | 0.6 | 110 | 0 |
| 17 | 16 | 45 | 0.8 | 110 | 0 |
| 18 | 16 | 45 | 1.0 | 110 | 0 |
| 19 | 16 | 34 | 0.5 | 90 | 24 |
| 20 | 16 | 34 | 0.5 | 100 | 24 |
| 21 | 16 | 34 | 0.5 | 110 | 24 |
| 22 | 16 | 34 | 0.5 | 130 | 24 |
| 23 | 16 | 34 | 0.5 | 150 | 24 |
| 24 (=9) | 16 | 34 | 0.5 | 110 | 0 |
| 25 | 16 | 34 | 0.5 | 110 | 2 |
| 26 | 16 | 34 | 0.5 | 110 | 4 |
| 27 | 16 | 34 | 0.5 | 110 | 6 |
| 28 | 16 | 34 | 0.5 | 110 | 16 |
| 29 (=21) | 16 | 34 | 0.5 | 110 | 24 |

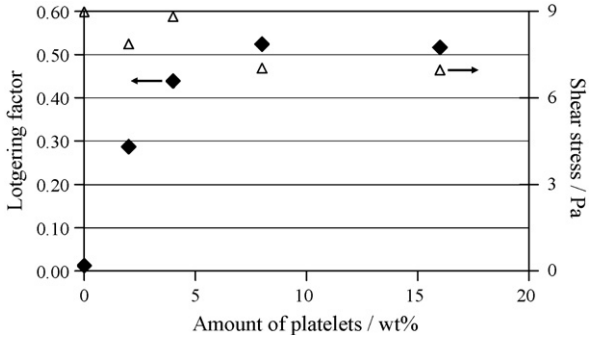


Fig. 3. The lotgering factor (♦) of the sintered piece (1650 °C) and the shear stress (△) during tape casting as function of the amount of platelets.

reason of this fairly low value, is that the intensity of the (0 0 6) peak in a powder sample is very low compared to those of other peaks, hence it is nearly impossible to reduce the other peaks to zero. Using Joshi's model, it showed that the average shear rate for the samples was nearly the same, hence small differences in rheological behaviour of the fluid were not responsible for differences in texture.

The alignment of the particles by the TGG process was confirmed in the SEM micrographs shown in Fig. 5. Fig. 5(a) and (b) shows the alignment of the template particles in the powder matrix after the tape casting process in the drawing direction. After sintering, as shown in the top view of the sintered sample in Fig. 5(c) and the cross-section view in Fig. 5(d), the template particles have grown at the expense of the smaller sized matrix powder and most of the matrix powder has disappeared.

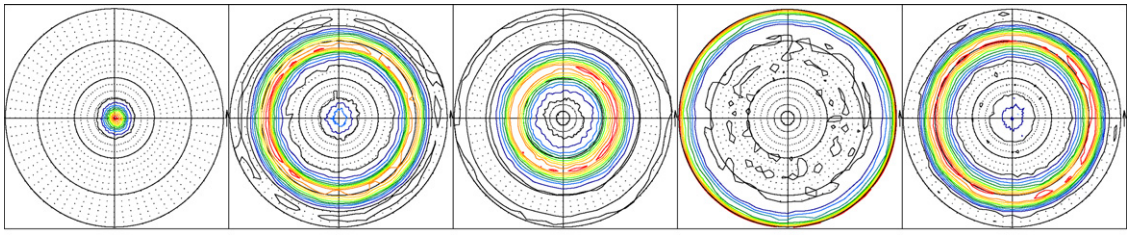

Fig. 4. Pole figures for the directions, from left to right: (0 0 6), (0 1 2), (1 0 4), (1 1 0), (1 1 2).

Table 3
The results for the lotgering factor resulting from X-ray measurements and λ and the average shear stress resulting from Joshi's model.

| | # | Lotgering factor | Average shear stress (Pa) | λ |
|---|---|---|---|---|
| % platelets series | 1 | 0.012 | 9.0 | 3.7 |
| | 2 | 0.287 | 7.9 | 3.3 |
| | 3 | 0.439 | 8.8 | 3.6 |
| | 4 | 0.524 | 7.0 | 3.0 |
| | 5 | 0.516 | 7.0 | 3.0 |
| Carrier tape speed series | 6 | 0.195 | 2.9 | 1.5 |
| | 7 | 0.329 | 4.3 | 2.0 |
| | 8 (=6) | 0.516 | 4.9 | 2.2 |
| | 9 | 0.408 | 5.4 | 2.4 |
| | 10 | 0.404 | 6.3 | 2.7 |
| | 11 | 0.388 | 7.1 | 3.0 |
| Gap heights series | 12 | 0.501 | 20.5 | 9.6 |
| | 13 | 0.530 | 11.0 | 5.4 |
| | 14 | 0.454 | 7.1 | 3.7 |
| | 15 (=10) | 0.404 | 5.0 | 2.7 |
| | 16 | 0.324 | 3.8 | 2.2 |
| | 17 | 0.304 | 2.4 | 1.6 |
| | 18 | 0.378 | 1.6 | 1.2 |
| Solid loading series | 19 | 0.443 | 5.1 | 2.3 |
| | 20 | 0.517 | 5.5 | 2.5 |
| | 21 | 0.567 | 5.6 | 2.5 |
| | 22 | 0.671 | 8.2 | 3.4 |
| | 23 | 0.512 | 8.9 | 3.7 |
| Deairing series | 24 (=9) | 0.408 | 5.4 | 2.4 |
| | 25 | 0.476 | 7.3 | 3.1 |
| | 26 | 0.445 | 5.7 | 2.5 |
| | 27 | 0.456 | 5.9 | 2.6 |
| | 28 | 0.510 | 5.3 | 2.4 |
| | 29 (=21) | 0.567 | 5.7 | 2.5 |

The influence of the carrier tape speed on the lotgering factor and the average shear stress is shown in Fig. 6. Although Joshi's model does not explicitly give the shear stress as a function of the carrier tape speed, the constant λ increases with higher carrier tape speed. As expected,[14] a higher carrier tape speed results in a higher alignment of the platelets, indicated by a higher lotgering factor for the sintered part. A slight drop can be observed at if the carrier tape speed exceeds 40 cm/min. Although this drop is not significant, it could indicate that higher speed results in lower orientation, since at higher speed the alignment time, the time a particle experiences shear stress, is lower. Although unlikely,[13,16] (localized) turbulence in the flow due to higher casting speed may be another factor.

Fig. 6 shows that the value of the lotgering factor at a carrier tape speed of 30 cm/min is higher than the other lotgering factors and that the average shear stress was higher. This specific sample is the same as in the first series in which the samples were deaired for 24 h, while in this second series the slurry was cast immediately after preparation. This prompted the investigation into the influence of the deairing time on the lotgering factor, the results of which are shown in Fig. 7. The graph shows that with increasing deairing time the lotgering factor increases, confirming that the aberration found in Fig. 6 is a real effect. Even though the shear stress decreases slightly with increasing deairing time, this does not likely explain the large difference in lotgering factor. A possible explanation might be found in the presence of air which provides pockets for the platelets to easily rotate after alignment.

The influence of the gap height on the lotgering factor and the average shear rate is depicted in Fig. 8. With the exception of a gap height of 0.2 mm, which resulted in dewetting, there is a decrease in the lotgering factor up to 0.6 mm levelling off at 0.8 mm and increase for 1.0 mm. The levelling off can be explained by the influence of the gap height $h_0$ on the constant λ. An increase in $h_0$ results in an decrease in λ, although not proportionally. As shown in Fig. 8 the shear stress levelled off at larger gap heights accounting for the levelling off of the lotgering factor at larger gap heights, although it does not account for the increase at 1.0 mm. This increase cannot be satisfactorily be explained at this time. The thickness of the samples itself after sintering increases linearly with the gap height, as expected.

The influence of the viscosity has been studied by changing the solid loading of the slurry; a higher solid loading results in a higher viscosity leading to a higher shear rate.[14] Apart from the sample with 90 g of alumina powder, which resulted in dewetting, all suspensions were successfully tape cast. The solid loading was limited to 150 g, since higher loading requires extra water in the first step to be able to disperse the powder. The dispersant concentration for all suspensions was kept at 2.0 wt% of the alumina powder. The results for this series of experiments

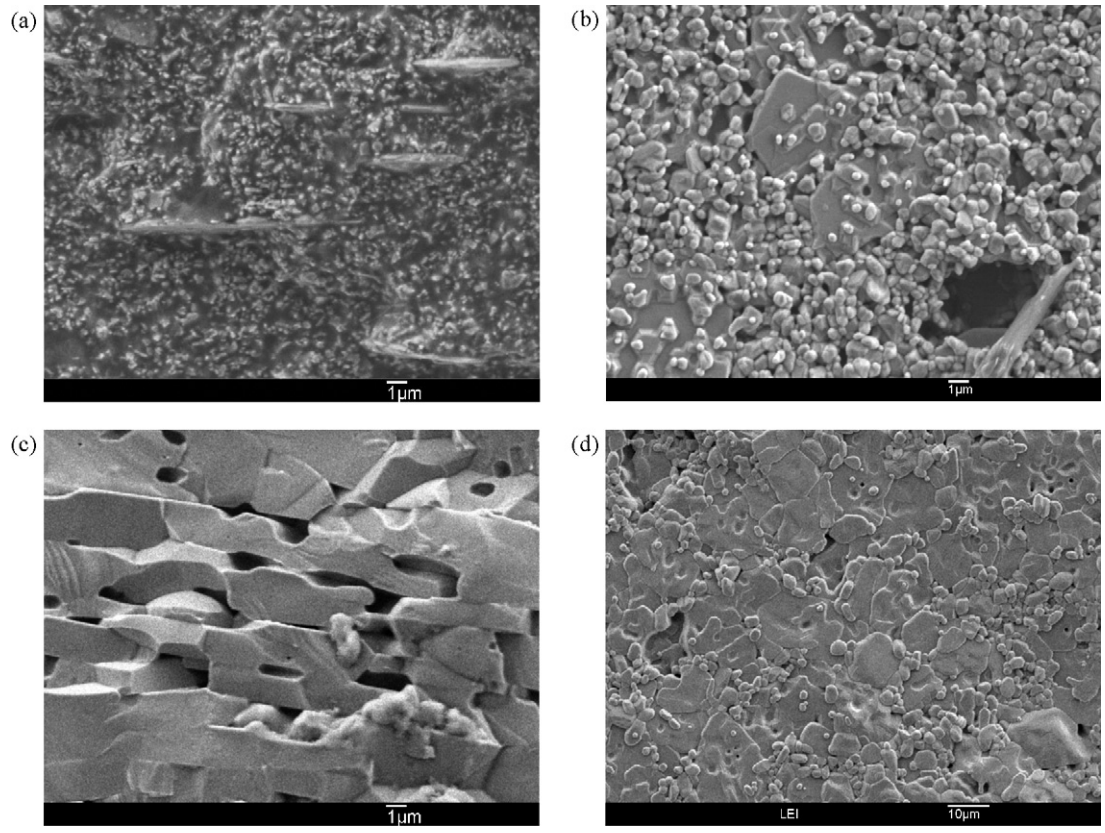


Fig. 5. SEM micrographs of (a) fractured cross-section of the green tape, (b) top surface of the green tape, (c) fractured cross-section of the sintered tape and (d) top surface of the sintered tape. The images are made on sample #5 with a lotgering factor of 0.524 after sintering.

are shown in Fig. 9. It clearly shows an increase in lotgering factor and shear stress with an increase in powder loading. Above 130 g powder/batch, the lotgering factor decreases, even though the shear stress increases. The increase in viscosity also means that deairing the slurry is harder, which as shown before has a large influence on the lotgering factor. Another important factor may be that the increase in viscosity makes aligning the templates harder, since a higher viscosity means more resistance to rotation of particles. Nevertheless, this is countered by the increase in shear rate, which should result in a higher lotgering factor,[14] making it likely that the drop in lotgering factor is the result of air in the suspension.

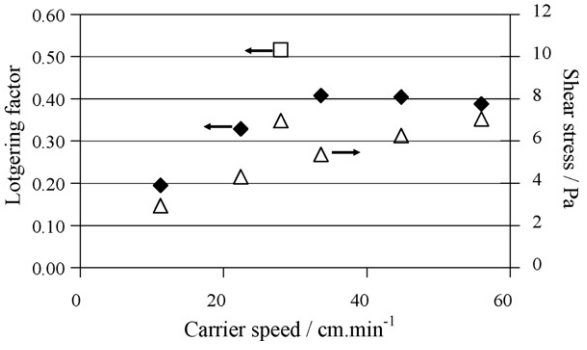


Fig. 6. Influence of the carrier tape speed on the lotgering factor of the sintered piece (1650 °C). The black diamonds (♦) were not deaired, the open square (□) was deaired for 24 h. The right axis shows the corresponding shear stress (△) according to Joshi's model.

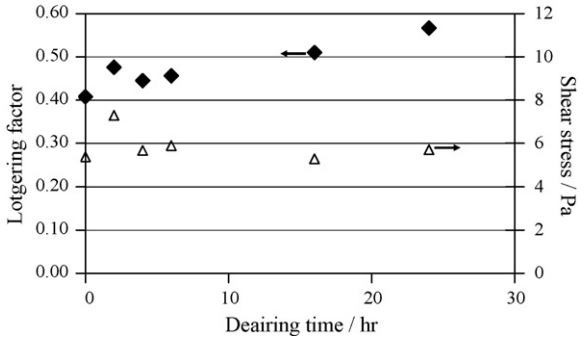


Fig. 7. The influence of the deairing time on the lotgering factor (♦) and the shear stress (△) during tape casting.

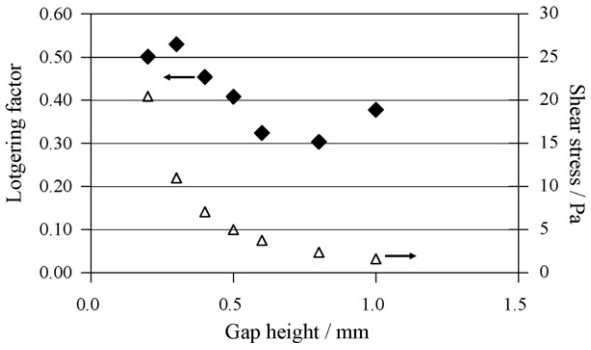


Fig. 8. The influence of the gap height on the lotgering factor (♦) of the sintered piece (1650 °C). The right axis gives the shear stress (△) as function of the gap height according to Joshi's model.

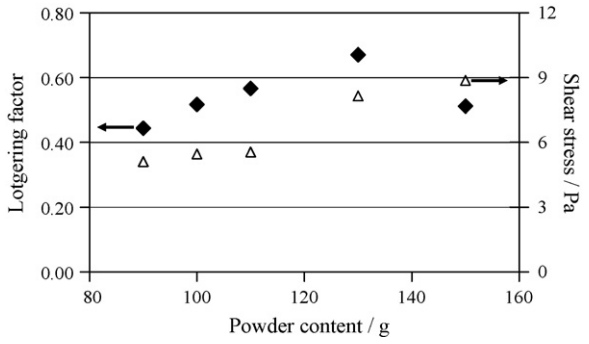


Fig. 9. Influence of the powder content on the lotgering factor (♦) and the shear stress according to Joshi's model (△).

## 5. Conclusions

The influence of the most important tape cast process parameters on the degree of orientation after templated grain growth of alumina have been studied and quantified. The increase of the platelets concentration resulted in an increase in the lotgering factor, in line with Joshi's model. For the carrier speed an increase was seen, however, if the carrier tape speed is too high, the particles have less time to align and possibly too short for full alignment. The influence of the gap height did not follow expectations; after an initial decrease, the lotgering factor levels and increases with a larger gap height. This was partly be explained using Joshi's model.

It was observed that the deairing time has a large influence on the lotgering factor; longer deairing times result in larger lotgering factors. It is likely that the small residual pockets of air provide the possibility for the template particles to rotate after alignment.

The lotgering factor is also increased by an increase in powder content. The resulting increase in viscosity yields higher shear stresses, giving better alignment for the particles. However it was found that if the powder content is raised too much, the lotgering drops due to the increased problem of deairing the slurry.

Overall it was shown that Joshi's model can be used to explain the effects of tape casting parameters on the alignment.

## Acknowledgement

This research is funded by the IWT project PROMAG (no. 060056).

## References

1. Messing, G. L., Trolier-McKinstry, S., Sabolsky, E. M., Duran, C., Kwon, S., Brahmaroutu, B. *et al.*, Templated grain growth of textured piezoelectric ceramics. *Crit. Rev. Solid State*, 2004, **29**, 45–96.
2. Okazaki, K., Igarashi, H., Nagata, K., Yamamoto, T. and Tashiro, S., Processing, microstructure, and properties of grain-oriented ferroelectric ceramics. *IEEE Trans. Ultrason. Ferroelectr. Freq. Control*, 1986, **33**, 328–337.
3. Suzuki, T. S., Uchikoshi, T. and Sakka, Y., Control of texture in alumina by colloidal processing in a strong magnetic field. *Sci. Technol. Adv. Mater.*, 2006, **7**, 356–364.
4. Sakka, Y., Suzuki, T. S. and Uchikoshi, T., Fabrication and some properties of textured alumina-related compounds by colloidal processing in high-magnetic field and sintering. *J. Eur. Ceram. Soc.*, 2008, **28**, 935–942.
5. Brosnan, K. H., Messing, G. L., Meyer, R. J. and Vaudin, M. D., Texture measurements in <001> fiber-oriented PMN-PT. *J. Am. Ceram. Soc.*, 2006, **89**, 1965–1971.
6. Seabaugh, M. M., Kerscht, I. H. and Messing, G. L., Texture development by templated grain growth in liquid-phase-sintered alpha-alumina. *J. Am. Ceram. Soc.*, 1997, **80**, 1181–1188.
7. Suvaci, E., Seabaugh, M. M. and Messing, G. L., Reaction-based processing of textured alumina by templated grain growth. *J. Eur. Ceram. Soc.*, 1999, **19**, 2465–2474.
8. Wada, S., Takeda, K., Muraishi, T., Kakemoto, H., Tsurum, T. and Kimura, T., Preparation of [1 1 0] grain oriented barium titanate ceramics by templated grain growth method and their piezoelectric properties. *Jpn. J. Appl. Phys.*, 2007, **1**(46), 7039–7043.
9. Suvaci, E., Oh, K. S. and Messing, G. L., Kinetics of template growth in alumina during the process of templated grain growth (TGG). *Acta Mater.*, 2001, **49**, 2075–2081.
10. Sakatani, Y., Grosso, D., Nicole, L., Boissiere, C., Soler-Illia, G. J. d. A. A. and Sanchez, C, Optimised photocatalytic activity of grid-like mesoporous $TiO_2$ films: effect of crystallinity, pore size distribution, and pore accessibility. *J. Mater. Chem.*, 2006, **16**, 77–82.
11. Watanabe, H., Kimura, T. and Yamaguchi, T., Particle orientation during tape casting in the fabrication of grain-oriented bismuth titanate. *J. Am. Ceram. Soc.*, 1989, **72**, 289–293.
12. Joshi, S. C., Lam, Y. C., Boey, F. Y. C. and Tok, A. I. Y., Power law fluids and Bingham plastics flow models for ceramic tape casting. *J. Mater. Process. Technol.*, 2002, **120**, 215–225.
13. Kim, H. J., Krane, M. J. M., Trumble, K. P. and Bowman, K. J., Analytical fluid flow models for tape casting. *J. Am. Ceram. Soc.*, 2006, **89**, 2769–2775.
14. Iverson, B., Kim, H. J., Slamovich, E. and Bowman, K., Texture evolution in tape cast lead metaniobate. *J. Eur. Ceram. Soc.*, 2008, **28**, 863–869.
15. Pitchumani, R. and Karbhari, V. M., Generalized fluid-flow model for ceramic tape casting. *J. Am. Ceram. Soc.*, 1995, **78**, 2497–2503.
16. Chou, Y. T., Ko, Y. T. and Yan, M. F., Fluid-flow model for ceramic tape casting. *J. Am. Ceram. Soc.*, 1987, **70**, C280–C282.
17. Itahara, H., Tani, T., Nomura, H. and Matsubara, H., Computational design for grain-oriented microstructure of functional ceramics prepared by templated grain growth. *J. Am. Ceram. Soc.*, 2006, **89**, 1557–1562.
18. Jing, X., Li, Y., Yang, Q., Zeng, J. and Yin, Q., Influence of different templates on the textured $Bi_{0.5}(Na_{1-x}K_x)_{0.5}TiO_3$ piezoelectric ceramics by the reactive templated grain growth process. *Ceram. Int.*, 2004, **30**, 1889–1893.
19. Wada, K., Kakimoto, K.-i. and Ohsato, H., Control of temperature coefficient of resonant frequency in $Ba_4Sm_{9.33}Ti_{18}O_{54}$ ceramics by templated grain growth. *Sci. Technol. Adv. Mater.*, 2005, **6**, 54–60.
20. Gao, F., Hong, R.-z., Liu, J.-j., Yao, Y.-h. and Tian, C.-s., Effect of different templates on microstructure of textured $Na_{0.5}Bi_{0.5}TiO_3$–$BaTiO_3$ ceramics with RTGG method. *J. Eur. Ceram. Soc.*, 2008, **28**, 2063–2070.
21. Jones, J. L., Iverson, B. J. and Bowman, K. J., Texture and anisotropy of polycrystalline piezoelectrics. *J. Am. Ceram. Soc.*, 2007, **90**, 2297–2314.
22. Wada, K., Kakimoto, K.-i. and Ohsato, H., Dielectric anisotropy and sinterability improvement of $Ba_4Nd_{9.33}Ti_{18}O_{54}$ textured ceramics. *J. Eur. Ceram. Soc.*, 2006, **26**, 1899–1902.
23. Snel, M. D., de With, G., Snijkers, F., Luyten, J. and Kodentsov, A., Aqueous tape casting of reaction bonded aluminium oxide (RBAO). *J. Eur. Ceram. Soc.*, 2007, **27**, 27–33.
24. Snel, M. D., Snijkers, F., Luyten, J., Kodentsov, A. and de With, G., Tape casting and reaction sintering of titanium–titanium oxide–nickel oxide mixtures. *J. Eur. Ceram. Soc.*, 2008, **28**, 1185–1190.
25. Bitterlich, B., Lutz, C. and Roosen, A., Rheological characterization of water-based slurries for the tape casting process. *Ceram. Int.*, 2002, **28**, 675–683.
26. Lotgering, F. K., Topotactical reactions with ferrimagnetic oxides having hexagonal crystal structures. *J. Inorg. Nucl. Chem.*, 1959, **9**, 113–123.